JOURNAL OF PROPULSION AND POWER
Vol. 15, No. 1, January–February 1999

# Droplet Spacing on Drag Measurement and Burning Rate for Isothermal and Reacting Conditions

J. F. Virepinte,* O. Adam,† G. Lavergne,‡ and Y. Biscos§
*ONERA, BP 4025-31055 Toulouse CEDEX, France*

**To understand the effects of droplet interaction on the drag coefficient and vaporization process, our experiment investigated the nonreacting and combustion history of a single stream of monosized droplets. Continuous monosized streams of fuel droplets were injected into quiescent surrounding air. An electronic device designed to modulate the droplet spacing $C$ (ratio of interdroplet spacing to droplet diameter) was used. Measurements of droplet diameter, droplet velocity, and droplet temperature were performed using nonintrusive laser interoferometry. Ethanol was used as the simulation fluid throughout the experiment. The droplet stream was investigated in cold conditions to study the influence of droplet spacing on the drag coefficient. The data compiled for an extensive range of parameters ($Re$, droplet spacing) were compared with previous correlations from the literature. We propose a new correlation that improves the prediction of the drag coefficient for a large range of spacing parameter $2 < C < 40$. For reacting conditions the droplet stream was ignited by a heated coil. The results of the first trial do not agree with the correlation established for cold conditions, therefore we formulated a new one valid for burning droplets. We also examine the effects of interaction in accordance with the spacing parameter. These results show that the classical "$D^2$ law" does not apply rigorously for interacting droplets, and so a corrective factor for burning rate was determined.**

## Nomenclature

$C$ = spacing parameter
$C_d$ = drag coefficient of a droplet
$D$ = fuel molecular diffusivity in air
$D_g$ = droplet diameter
$f$ = excitation frequency
$\dot{m}$ = evaporating rate
$Pr$ = droplet Prandtl number
$Q$ = liquid feed rate
$R$ = radial distance
$Re_g$ = particular Reynolds number
$S_g$ = center-to-center droplet spacing
$T_{boil}$ = droplet boiling temperature
$T_g$ = droplet temperature
$T_{inj}$ = injection droplet temperature
$t$ = time
$V$ = velocity of surrounding gas
$V_g$ = droplet velocity
$\alpha$ = Mie parameter
$\lambda$ = light wavelength
$\mu$ = dynamic viscosity of surrounding gas
$\rho$ = density of surrounding gas
$\Phi_0$ = orifice diameter

*Subscripts*
iso = isolated droplet
0 = initial droplet condition before droplet deviation

## Introduction

MANY practical devices such as diesel, gas turbine, and rocket engines use liquid fuel sprays in their combustion chamber to produce power for a variety of applications. Fuel sprays consist of individual fuel droplets less than 200 $\mu$m in diameter. Combusting sprays involve many physical processes, such as drop–drop interaction, drop–gas phase interaction, and drop vaporization. Each of these physical processes are coupled and cannot be accurately modeled for computational fluid dynamics (CFD) applications. For that reason many of them are being studied experimentally to give a complete understanding of the individual processes involved in the combustion of sprayed liquid fuel. These studies have led the laboratory to develop a two-phase flow numerical module called Lagrangian simulation of dispersion (LSD).[1] This module is coupled with a gas-phase numerical code including a $k$-$\varepsilon$ model for the turbulence. This code has historically been applied to two-phase burning sprays in turbojet combustion chambers, in the case of dilute sprays. Now, this code is being extended to the three-dimensional two-phase flows, including burning droplets and dense sprays. In the case of dense spray, the interactions between the two phases (two-way coupling) and the interactions between the droplets are the dominating processes (four-way coupling).

The aim of this paper is to present the results of a basic experiment on droplet interaction in a dense linear spray. A stream of monosized droplets is generated by a vibrating orifice generator. The basic experiment allows us to precisely quantify the evolution of the drag coefficient and the droplet burning rate for various droplet spacings.

## Experimental Setup

### Droplet Generator

The experiment is set up around a monosized droplet generator in which a piezoceramic induces Rayleigh instability on a solid liquid stream, thereby breaking it up into a series of monodispersed droplets (Fig. 1).[2] By appropriate choice of $\Phi_0$, $f$, and $Q$, each droplet has the same initial conditions and undergoes the same series of events along its trajectory. $D_g$, $V_g$, and $S_g$ are defined by the following relations:

$$D_g = (6 \cdot Q/\pi \cdot f)^{1/3} \quad (1)$$

$$V_g = 4 \cdot Q/\pi \cdot \phi_0^2 \quad (2)$$

Received Aug. 26, 1997; revision received June 9, 1998; accepted for publication June 13, 1998. 

*Graduate Student, CERT/DMAE. E-mail: virepinte@onecert.fr.
†Graduate Student, CERT/DMAE.
‡Research Engineer, Head of Heterogeneous Multiphase Flow Unit, CERT/DMAE. E-mail: lavergne@onecert.fr.
§Research Engineer, CERT/DMAE. E-mail: biscos@onecert.fr.

$$S_g = V_g/f \quad (3)$$

The droplet size ranges from 70 to 200 $\mu$m, and the droplet velocity varies from 5 to 15 $ms^{-1}$. Because of the principle of monodispersed droplet formation, the initial droplet spacing ranges between three and seven droplet diameters. This device also allows the heating/cooling of the injected liquid.

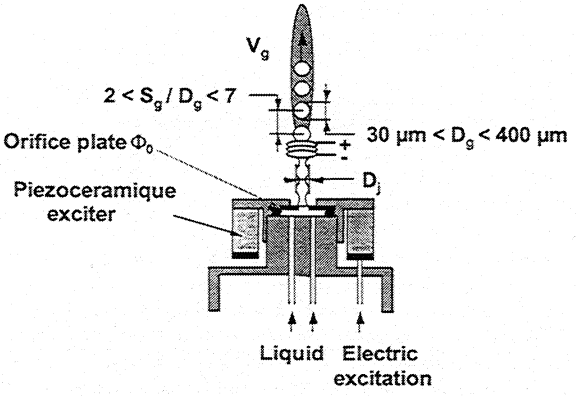


**Fig. 1 Monosized droplet generator.**

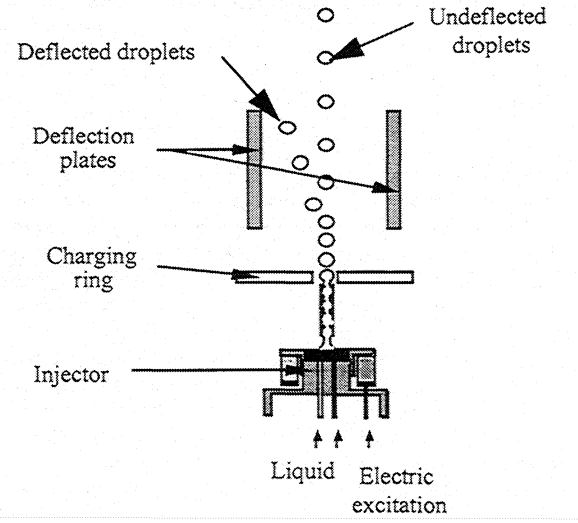


**Fig. 2 Electrostatic droplet deflector.**

### Electrostatic Droplet Deflector

To increase the droplet spacing (Fig. 2), an electrostatic droplet deflector has been designed.[3,4] The number of deflected droplets is adjustable; e.g., a maximum droplet spacing on the order of 50 droplet diameters is obtainable.

The operating mode of the device is as follows: the liquid jet is circumscribed by a ring electrode at the point where droplets are created. A voltage pulse of positive polarity (50–350 V) is applied to the ring at a fraction of the excitation frequency. Therefore, a droplet crossing the charging ring captures a negative charge and can be electrostatically deflected. The droplet stream passes between two plates charged to opposite polarity voltages, the charged droplets are extracted from the main stream and collected by a drain. As a result we are able to investigate a stream with large spacing. The analysis of burning droplet stream is also possible. The monodispersed droplet stream may be ignited by a heated coil located downstream from the electrostatic droplet deflector. After ignition the droplet is surrounded by a laminar diffusion flame.

## Measuring Techniques

To obtain the drag coefficient, evaporation rate, and burning rate, the droplet size, velocity, and temperature had to be measured simultaneously along the droplet path. The experimental setup is shown schematically in Fig. 3.

### Droplet Size Measurements

To measure the droplet size and temperature, a laser beam is focused at a location along the axis of the droplet stream.[2–5] The light path of a beam interacting with the droplet surface at the angle of incidence $\tau$ is shown in Fig. 4. At each interaction between a light ray and the droplet surface, the light is reflected or refracted. Light rays exiting the droplet stream experience a varied number of refractions and reflections with the droplet surfaces. This number is described as $p$, such that one reflection on the droplet surface is of the order $p = 0$. The ray that is refracted twice and leaves the droplet is of the order $p = 1$, etc. (Fig. 4).

The rays of the order 0 and 1 generate an interference pattern in the forward direction. Because of the high frequency of the droplets, a stationary light pattern can be observed. The intensity distribution of the scattered light is described by the equations of Mie's theory, which introduces the dimensionless Mie parameter

$$\alpha = \pi D_g/\lambda \quad (4)$$

where $\lambda$ is the light wavelength.[6] For Mie parameter $\alpha \gg 1$, equations of geometrical optics can be used instead of the more

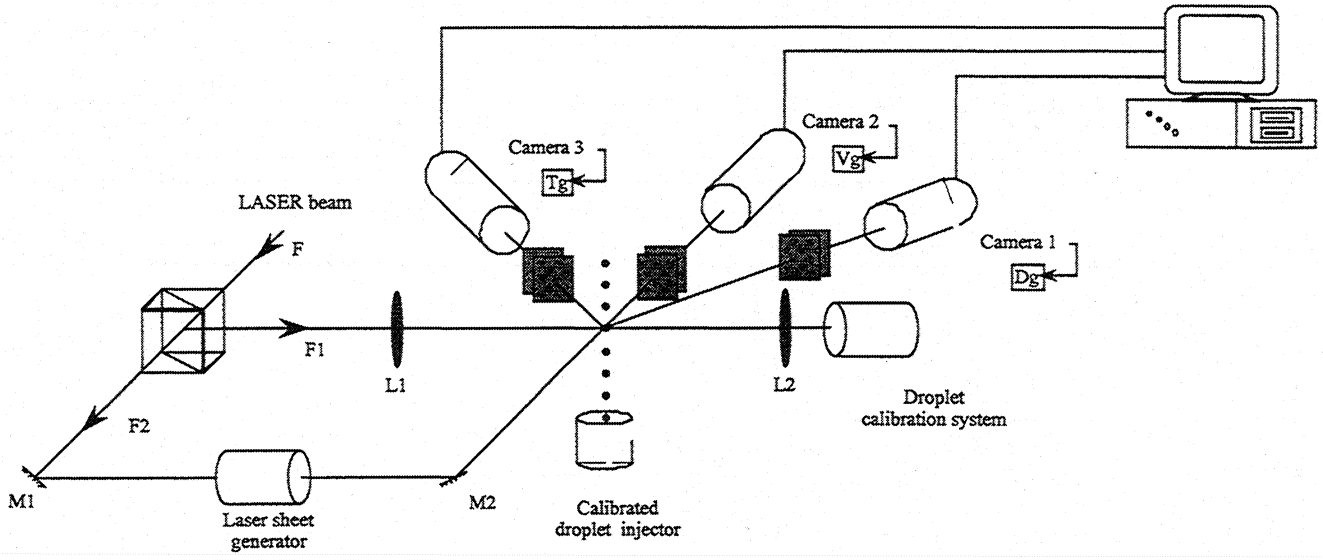


**Fig. 3 Experimental setup.**

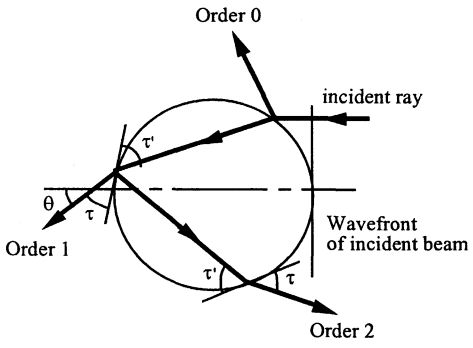


**Fig. 4 Light path through a droplet.**

complicated Mie theory to calculate the intensity distribution of the scattered light. However, this simplification fails close to the forward direction and near the rainbow angle and, thus, is only valid for angles between 30 and 80 deg. As the droplets and the angle in the present experiment fulfill these conditions, the signal is recorded by a linear charge-coupled device (CCD) array (1) (Fig. 3). The angular spacing is measured between two interference maxima to calculate the droplet size. With this method the determination of the droplet size is done with an accuracy of 1%.[7]

### Droplet Temperature Measurements

For a refraction order larger than 1, rainbow phenomena are observed. However, only the first rainbow created by the rays of order 2 is strong enough to be easily detected. Using geometrical optics, one obtains the result that the rainbow angle is a function of the refractive index of the liquid used and of the order of the rays only. The refractive index is a function of density that is dependent on temperature. For this reason the droplet temperature can be determined by measuring the rainbow angle. The light of the first rainbow is recorded by another linear CCD array (Fig. 3).[3] If the shift of the first rainbow is larger than the width of the linear CCD array, the linear CCD array can be moved precisely and the total shift of the rainbow relative to the initial position can be calculated.

We used a calculation method by means of the Airy/Walker theory that enables the computation of the refractive index of the droplet from the rainbow angle.[8] For this calculation method, the droplet diameter, the refractive index/temperature relationship, and the angular position of the rainbow must be known. The refractive index/temperature relationship for ethanol of 90% purity was obtained experimentally using a refractometer at the wavelength of 632.8 nm (He–Ne laser). To obtain the angular position, a mirror was located precisely at the focal point. The calibration was conducted by rotating the mirror to sweep the CCD array pixels with a laser beam. Finally, the droplet temperature can be determined with an uncertainty of approximately 4 K.[6]

### Droplet Velocity Measurements

To measure the droplet velocity, we used a second laser beam. It crossed through a cylindrical lens to produce a laser sheet.[9] This laser sheet was used to illuminate the droplet stream at the same location where the size measurement is performed. Therefore, more than one droplet is present within the laser sheet at any given instant. The spacing between the droplets plays the role of a punctual light source. In a perpendicular plane to the optical axis of the illumination, stationary Young's fringes can be observed. These fringes are recorded by a third CCD array (Fig. 3).[2] By measuring the fringe spacing, we obtain the droplet spacing. Knowledge of the excitation frequency of the droplet generator is necessary to calculate the droplet velocity. This technique is only valid for monodispersed droplet streams. However, for a droplet spacing greater than 7, Young's fringes cannot be observed. Therefore, we used a video camera and image-processing technique to determine the droplet velocity. The determination of the droplet velocity was done with an accuracy of 1%.[6]

By simultaneously measuring droplet size, velocity, and temperature at different locations downstream from the injector, the temporal evolution of these parameters can be determined either with or without combustion.

## Results

The results are divided in two groups. Firstly, we investigated a droplet stream in cold conditions to study the influence of the droplet interaction on the drag coefficient without the evaporation process. We compared our results with the existing available models in the literature. Then we studied the temporal evolution of the droplet diameter and the corrective factor of the burning rate for various spacing parameters.

### Cold Conditions

*Theoretical Drag Coefficient*

The drag coefficient of an isolated droplet is given by the following equation[10]:

$$C_d = \begin{cases} \dfrac{24}{Re_g}(1 + 0.15Re_g^{0.687}) & \text{for} \quad Re_g < 1000 \\ 0.438 & \text{for} \quad Re_g \geq 1000 \end{cases} \tag{5}$$

$$Re_g = \frac{\rho D_g(V - V_g)}{\mu} \tag{6}$$

To take into account the droplet interaction, some works were carried out by Zhu et al.[11] and Mulholland et al.[12] They determined that the drag coefficient is a function of $Re_g$ and $C$. These correlations will be compared with our experimental results in a later subsection.

*Experimental Drag Coefficient*

$C_d$ is determined from the equation of the motion of a spherical droplet

$$\frac{dV_g}{dt} = \frac{3\rho C_d}{4\rho_l D_g}\|V - V_g\|(V - V_g) + g \tag{7}$$

The droplet stream induces a small air entrainment but it is assumed close to zero $V \ll V_g$. The relative velocity is equal to $V_g$. The physical properties are calculated from the correlation given by Beard.[13] The drag coefficient was measured along the droplet stream. The diameter and velocity profiles were curve fitted using a first-order linear regression method. This correlation fits the data within ±5%.

*Comparison Between the Literature and Experimental Results*

We compared our results with Zhu et al.'s[11] and Mulholland et al.'s[12] correlations. For low spacing parameter values, both correlations were not in agreement with the experimental curve. They overpredicted the drag coefficient of the droplets. It is not surprising for the Zhu et al.'s correlation because their study was limited to two interacting particles in line. This configuration differs considerably from the case of a monodispersed droplet stream. Moreover Zhu et al.'s correlation was limited to a spacing parameter lower than 8. Mulholland et al.'s model overestimated the experimental values until a spacing parameter of about 20. For a spacing parameter much larger, Mulholland et al.'s model does not have the same tendency as our experimental results. The differing results between our work and Mulholland et al.'s may be a result of the experimental arrangement. Mulholland et al. studied a monodispersed droplet stream injected horizontally in a steady air environment. Therefore, the droplet trajectories were not rectilinear as in our experiment and the droplet drag coefficient may be different for several $C$.

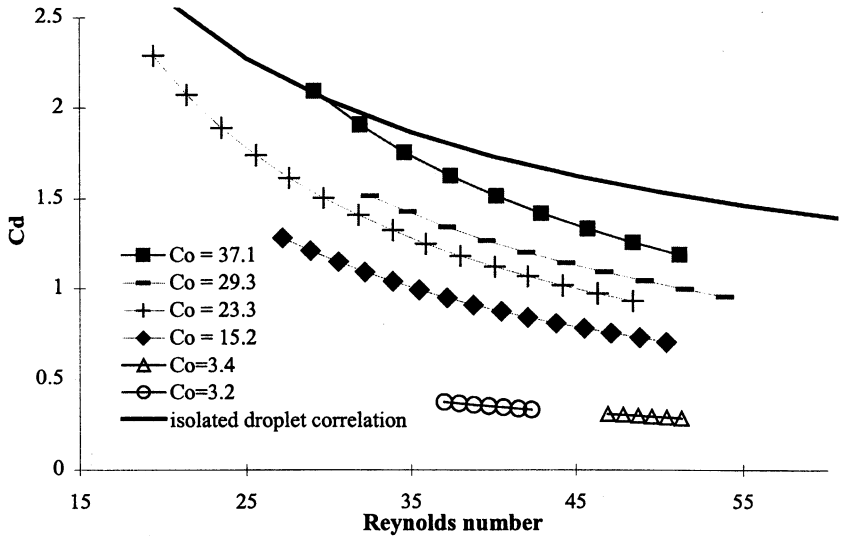


**Fig. 5 Experimental results and isolated droplet law for the drag coefficient.**

Those differences and the fact that the isolated droplet correlation [Eq. (5)] and our results do not have the same slope for large droplet spacings led us to determine a new expression of the drag coefficient. Using the least-square method, this equation was obtained over a wide range of spacing parameters $2 < C < 40$ and for a Reynolds number ranging from $2.0 \times 10^1$ to $7.5 \times 10^1$. The regression coefficient was 0.98:

$$Cd = 53.2Re_g^{-1.524}C^{0.6} \tag{8}$$

The results are presented in Fig. 5. $C_0$ is the initial droplet spacing. Its influence on the drag coefficient appears clearly. The discrepancy between the slope of the isolated droplet law and the experimental results for large droplet spacing ($C_0$ = 37) prompted us not to determine a form that asymptotes with Eq. (5) for infinite droplet spacings.

### Combustion Conditions

*Experimental Correlation*

Several works have been performed to take into account the droplet interaction in the case of evaporation. For example, Chiang and Sirignano[14,15] have studied two and three droplets that follow each other in a hot laminar flow. Unfortunately, we have an incomplete database on the evolution of the drag coefficient for several spacing parameters in the case of evaporating or burning droplets. On the other hand, the influence of evaporation was studied for isolated droplets by a large number of authors. In particular, Yuen and Chen[16] explained that the drag coefficient for evaporating droplets agrees with the standard curve of an isolated droplet if the Reynolds number is calculated at reference conditions

$$Re = \frac{\rho(T_a)\|V - V_g\|D_g}{\mu_m(T_{\text{ref}})} \tag{9}$$

where $\rho(T_a)$ is the density calculated at the surrounding temperature $T_a$, and $\mu_m$ is the dynamic viscosity of the mixture at a reference temperature estimated from the 1/3 rule established by Hubbard et al.[17] In the 1/3 rule, properties are evaluated at

$$T_{\text{ref}} = T_s + (T_a - T_s)/3 \tag{10}$$

and the mass fraction

$$Y_{\text{ref}} = Y_{Fs} + (Y_{F\infty} - Y_{Fs})/3 \tag{11}$$

where $T_s$ and $Y_{Fs}$ refer to the droplet surface, and $Y_{F\infty}$ to the freestream conditions. The dynamic viscosity must be calculated using the formula suggested by Wilke.[18] Using this expression, it is not necessary to take the effects of the mass-transfer number into account to calculate the drag coefficient. Initially, our aim was to obtain, if possible, a single expression of the drag coefficient for cold conditions and combustion. For this reason we used the reference conditions to determine it. As for the cold conditions, we considered that the relative velocity was equal to $V_g$. Moreover, the surrounding temperatures were determined using coherent anti-Stokes raman spectroscopy (CARS) measurements.[19,20]

The experimental results (Fig. 6) did not agree with those obtained for cold conditions, and so we determined a new expression for burning droplets in case of significant interaction ($C < 6$):

$$C_d = 1.53Re_g^{-0.67}C^{0.81} \tag{12}$$

The regression coefficient is 0.9. This correlation is defined for the following range of a particular Reynolds number $2 < Re_g < 20$ and spacing parameter $2 < C < 6$. This result will be very useful to simulate burning droplets trajectories in significant interaction into CFD codes.

*Comparison with $D^2$ Law*

Figure 7 shows the evolution of the experimental $D_g$ in combustion for several spacing parameters. The classical $D^2$ law is plotted as well:

$$(D/D_0)^2 = 1 - Kt \tag{13}$$

In this model it is assumed that the droplet is spherical and isolated, that the temperature is constant and uniform, and that all of the absorbed heat is used to evaporate the droplet. The physical properties of the air–vapor mixture around the droplet are calculated with the 1/3 rule.[14]

This law must be modified to take the convection effects into account [$K'$ replaces $K$ in Eq. (13)]:

$$K' = K(1 + 0.3Re_g^{0.5}Pr^{1/3}) \tag{14}$$

The diameter evolution is plotted in a classical representation vs the dimensionless time $t^*$

$$t^* = \frac{8\rho_m t_D \ell n(1 + B)}{D_{g0}^2\rho_g} \tag{15}$$

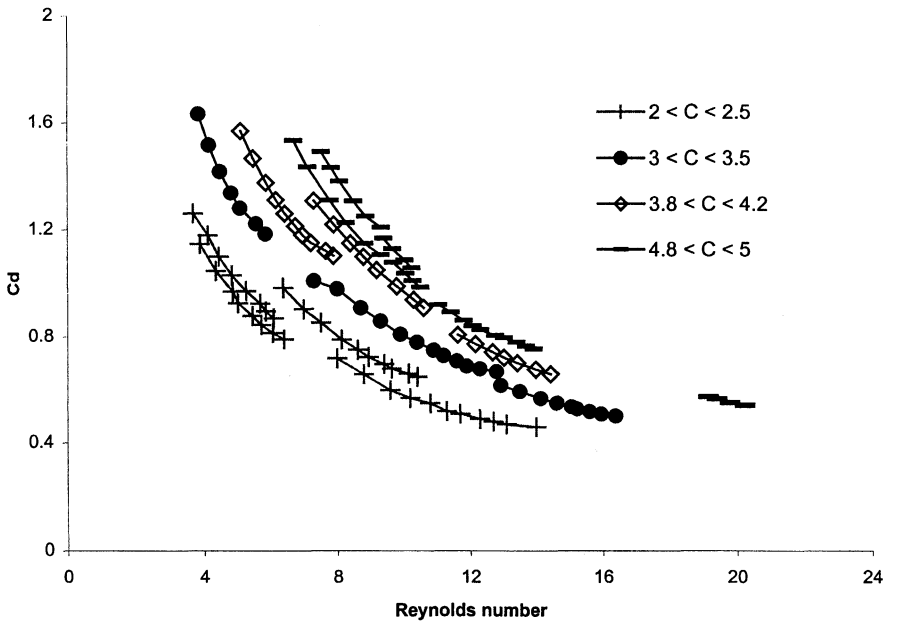


**Fig. 6 Dependence of the experimental results for burning droplets on the spacing parameter.**

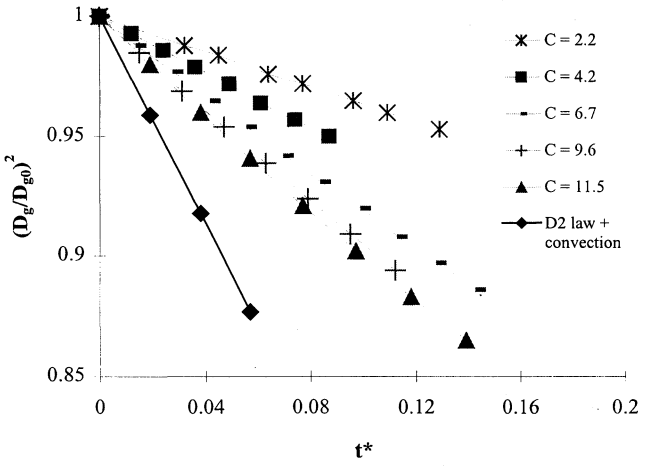


**Fig. 7 Droplet diameter evolution for several spacing parameters.**

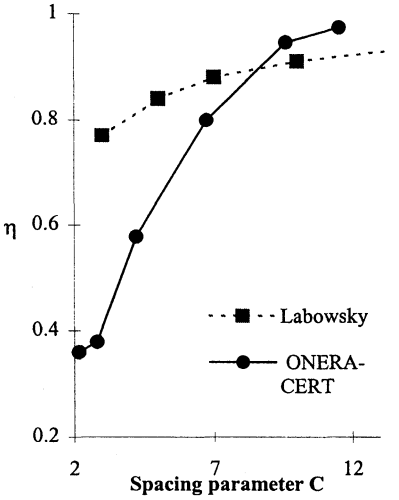


**Fig. 8 Dependence of the burning rate correction factor on *C*.**

where $D$ is the fuel molecular diffusivity in air, and $\rho_m$ are $\rho_g$ are the density of the mixture and the density of the droplet, respectively.[14] $B$ is the transfer number of Spalding, defined in combustion by

$$B = \frac{C_{pa}(T_\infty - T_g) + Q\upsilon Y_{0\infty}}{L_V} \tag{16}$$

$C_{pa}$ is the heat capacity of the air at the reference temperature, $T_\infty$ is the ambient temperature, $Q$ is the heat of combustion, $\upsilon$ is the stoichiometric coefficient, $Y_{0\infty}$ is the ambient mass rate of oxygen, and $L_V$ is the heat of vaporization.[14] One can notice that for a spacing parameter $C = 12$, the evolution of the diameter did not yet reach the isolated droplet curve. Moreover, an increasing spacing parameter induces a reduction of the heating time. The slope of these curves correlates directly to the corrective factor $\eta$ of the burning rate defined by Labowsky[21]:

$$\eta = \dot{m}/\dot{m}_{\text{iso}} \tag{17}$$

With the first experimental results we plotted the evolution of $\eta$ as a function of the spacing parameter in Fig. 8. Therefore, we can compare them to the numerical simulation of Labowsky for two burning droplets.[22] The effects of interaction are much more important in the experiments than in the simulation. This evolution will permit us to correct the burning rate of the droplets in numerical simulations.

## Conclusions

The experimental setup and the electrostatic droplet deflector were achieved. We defined a new correlation of the drag coefficient for interacting droplets. It improves the prediction of the coefficient drag to the transition between the high and low droplet interaction. The results concerning the droplet combustion show that an expression must be determined only for this regime.

The results of this study represent a first step in developing a technological base necessary to efficiently investigate droplet evaporation rate and drag coefficient by identifying some major trends resulting from $C$. These experimental results will constitute a benchmark for numerical code development and validation.

## Acknowledgments

This research is sponsored by the French Ministere of Defense (Service des Programme Aéronautiques). The Project

Monitor was Ormancey. The authors acknowledge A. Frohn and K. Anders of the Institut für Thermodynamik der Luft und Raumfahrt Stuttgart University for their assistance.

## References

[1]Beard, P., Bissieres, D., Lavergne, G., and Rompteaux, A., "Experimental and Numerical Studies of Droplet Turbulent Dispersion in Two-Phase Flows," *Proceedings of the 1994 ASME Fluids Engineering Division Summer Meeting* (Lake Tahoe, NV), FED Vol. 185, American Society of Mechanical Engineers, New York, 1994, pp. 15–22.

[2]König, G., Anders, K., and Frohn, A., "A New Light-Scattering Technique to Measure the Droplet Diameter of Periodically Generated Moving Droplets," *Journal of Aerosol Science*, Vol. 17, No. 2, 1986, pp. 157–167.

[3]Russo, R. E., Withnell, R., and Hieftje, G. M., "Simple and Inexpensive Design for an Isolated Droplet Generator Useful in Studies of Atomisation in Flames," *Applied Spectroscopy*, Vol. 35, No. 6, 1981, pp. 531–536.

[4]Warnica, W. D., Van Reenen, M., Renksizbulut, M., and Strong, A. B., "Charge Synchronization for a Piezoelectric Droplet Generator," *Review of Scientific Instrumemts*, Vol. 64, No. 8, 1993.

[5]Roth, N., Anders, K., and Frohn, A., "Refractive Index Measurements for the Correction of Particle Sizing Methods," 2nd International Congress on Optical Particle Sizing, Arizona State Univ., Tempe, AZ, March 1990.

[6]Mie, G., "Beiträge zur Optik Trüber Medien, Speziell Kolloidaler Metallösungen," *Annals of Physics*, Vol. 25, 1908, pp. 377–445.

[7]Adam, O., "Etude Expérimentale du Comportement des Gouttes en Régime d'Interaction," Ph.D. Dissertation, École Nationale Supérieure de l'Aéronautique et de l'Espace, France, 1997.

[8]Walker, J. D., "Rainbows from Single Drops of Water and Other Liquids," *American Journal of Physics*, Vol. 44, No. 5, 1976, pp. 421–433.

[9]Anders, K., Roth, N., and Frohn, A., "Simultaneous In-Situ Measurements of Size and Velocity of Burning Droplets," 4th Europäisches symposion partikelmeßtechnik, Nürnberg, Germany, 1989.

[10]Clift, R., Grace, J. R., and Weber, M. E., *Bubbles, Drops and Particles*, Academic, New York, 1978.

[11]Zhu, C., Liang, S. C., and Fan, L. S., "Particle Wake Effects on the Drag Force of an Interactive Particle," *International Journal of Multiphase Flow*, Vol. 20, No. 1, 1994, pp. 117–129.

[12]Mulholland, J. A., Srivastava, R. K., and Wendt, J. O. L., "Influence of Droplet Spacing on Drag Coefficient in Nonevaporating, Monodisperse Streams," *AIAA Journal*, Vol. 26, No. 10, 1988, pp. 1231–1237.

[13]Beard, P., "Modélisation Lagrangienne de la Dispersion et de l'Évaporation de Gouttes dans un Écoulement Instationnaire," Ph.D. Dissertation, École Nationale Supérieure de l'Aéronautique et de l'Espace, France, 1994.

[14]Chiang, C. H., and Sirignano, W. A., "Interacting, Convecting, Vaporizing Fuel Droplets with Variable Properties," *International Journal of Heat and Mass Transfer*, Vol. 36, No. 4, 1993, pp. 875–886.

[15]Chiang, C. H., and Sirignano, W. A., "Axisymmetric Calculation of Three-Droplet Interactions, Atomisation and Sprays," Vol. 3, 1993, pp. 91–107.

[16]Yuen, C., and Chen, L. W., "On Drag of Evaporating Liquid Droplets," *Combustion Science and Technology*, Vol. 14, 1976, pp. 147–154.

[17]Hubbard, G. L., Denny, V. E., and Mills, A. F., "Droplet Evaporation, Effects of Transient and Variable Properties," *International Journal of Heat and Mass Transfer*, Vol. 18, 1975, pp. 2588–1008.

[18]Wilke, C. R., "A Viscosity Equation for Gas Mixtures," *Journal of Chemical Physics*, Vol. 18, 1950, p. 517.

[19]Magre, P., Moreau, P., Collin, G., Borghi, R., and Pealat, M., "Further Studies by CARS of Premixed Turbulent Combustion in a High Velocity Flow," *Combustion and Flame*, Vol. 71, No. 2, 1988, pp. 147–168.

[20]Zhu, J. Y., and Dunn-Rankin, D., "Temperature Characteristics of a Combusting Droplet Stream," *24th Symposium on Combustion*, The Combustion Inst., Pittsburgh, PA, 1992, pp. 1473–1481.

[21]Labowsky, M., "Calculation of the Burning Rates of Interacting Fuel Droplets," *Combustion Science and Technology*, Vol. 22, 1980, pp. 217–226.

[22]Marberry, M., Ray, A. K., and Leung, K., "Effect of Multiple Particle Interactions on Burning Droplets," *Combustion and Flame*, Vol. 57, 1984, pp. 237–245.